Romanian Reports in Physics, Vol. 65, No. 3, P. 792–804, 2013

Dedicated to Professor Valentin I. Vlad's 70th Anniversary

NANOELECTRONICS ON A SINGLE ATOM SHEET

MIRCEA DRAGOMAN

National Institute for Research and Development in Microtechnology (IMT), P.O. Box 38-160, 023573 Bucharest, Romania

Received June 25, 2013

"Whatever you can do or dream you can, begin it.
Boldness has genius, power and magic in it".

Abstract. I will present my recent research concerning electronic devices on graphene. Graphene was discovered few years ago, and its amazing physical properties have ignited the hopes to reach THz frequencies with a single electronic device. So, high speed devices challenging Moore's law have emerged in the last years, opening the era of "beyond Moore law".

Key words: nanoelectronics, graphene, carbon nanotubes.

1. INTRODUCTION

Moore's law is the road map of electronic devices development over next decades [1]. However, the carbon nanomaterials and devices were changed the way in which we are thinking the electronic devices. Since the early 90's the research has been boosted by a new class of material based on organized aggregation of carbon atoms. Carbon nanotubes (CNT) discovered in 1991 [2], have been considered as key building element owing to their extremely promising electrical and mechanical properties.

Recently, in 2004 the isolation of a monoatomic thick aggregate of carbon atoms termed as graphene, has become one of the most studied subject in the area of applied physics, nanotechnology and nanoelectronics [3, 4] and also in engineering and application oriented research [5].

In fact both, CNT and graphene, are investigated from the manufacturing point of view, and from the experimental and theoretical perspective, to achieve large scale production guarantying high reproducibility and material purity levels via sophisticated production and characterization techniques [6, 7]. On the other hand a new theoretical understanding is being defined upon fundamental principles borrowed from classical and quantum physics [8, 9].

The graphene and CNT are extremely sensitive to external excitations such as electrical or magnetic field, mechanical forces, or electrochemical interactions with an external element. These peculiar characteristics are used to the discovery of an entire new class of devices, which combine at once electrical mechanical and biochemical functionalities in the same place [10,11].

2. THE PHYSICAL PROPERTIES OF GRAPHENE

Graphene is a monoatomic layer material with a thickness of only 0.34 nm consisting of carbon atoms in the sp^2 hybridization state. In graphene each carbon atom is covalently bonded to three others, such that the graphene lattice is a honeycomb composed of two interpenetrating triangular sublattices. Graphene is the first 2D material discovered and is the basic structure of other carbon-based materials, in particular of graphite, which results from stacked sheets of graphene, and of carbon nanotubes which could be regarded as rolled-up structures of a single or multiple graphene sheets [12].

The graphene was isolated for the first time by mechanically exfoliating graphite on a 300 nm SiO_2 layer deposited on a Si substrate [13]. Later, it was discovered that the control of the texturing of the substrate, will lead to the graphene-based devices *via* local strain creation through deformation of graphene [14].

The knowledge of the band structure of graphene is essential. The honeycomb structure of carbon atoms which constitute a graphene layer is represented in Fig. 1a. The reciprocal lattice has also a honeycomb shape and the first Brillouin zone and it ii is depicted in Fig. 1b, which is a hexagon with a length of $4\pi(3)^{-1/2}/3a$, where a = 0.14 nm is the carbon bond length. The points K and K' are essential because here the two triangular sublattices formed by the two lattice vectors $\mathbf{a_1}$ and $\mathbf{a}_2$ (see Fig. 1a) become separate to form the so called Dirac point.

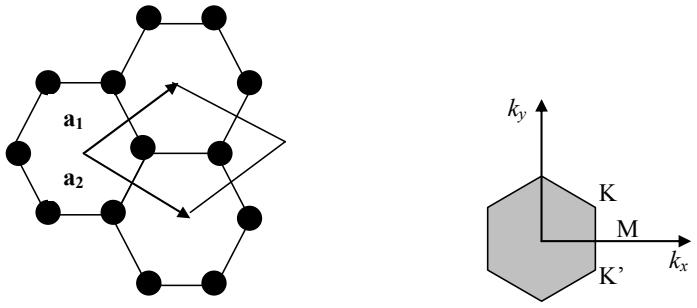

Fig. 1 – a) Graphene honeycomb lattice structure; b) its first Brillouin zone of the reciprocal lattice.

The dispersion relation of graphene is given by:

$$E(k) = \pm\gamma_0[1 + 4\cos(3^{1/2}k_x a/2)\cos(k_y a) + 4\cos^2(k_y a/2)]^{1/2}, \quad (1)$$

where $\gamma_0 = 3$ eV and is computed based on the tight-binging approximation. More details about this dispersion relation and its derivation are found in [15] and [16] and originates from Dirac equation describing carrier transport in graphene. Near the K and K' points equation (1) becomes:

$$E = \pm\hbar|\mathbf{k}|v_F, \quad (2)$$

where $\mathbf{k} = \mathbf{i}k_x + \mathbf{j}k_y$ is the wavenumber measured from K and K', v_F is the Fermi velocity of 10^6 m/s, and the positive (negative) sign is assigned to electrons (holes). The dispersion relation (1) is formed by two cones represented in Fig. 2.

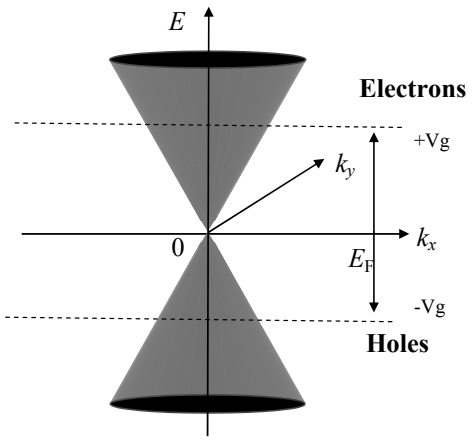

Fig. 2 – Graphene dispersion relation.

The relation (2) means that the effective mass of charge carriers is zero near Dirac point where the carrier density is 0, indicating us a ballistic transport of carriers, *i.e.* a weak interaction between the carriers and the lattice. The charge carriers propagate without collisions through graphene, *i.e.* balistically, with the velocity $v_F \cong c/300$, where c is the speed of light. In graphene the mean free-path of the carriers is 200–300 nm at room temperature, and this is a very large value compared to that of nanodevices fabricated with particle lithography such as e-beam or focused-ion beam with few nm features. So, graphene can be modeled as a 2D gas of massless carriers. The carriers either electrons or holes play an equal role in graphene, both having the same effective mass equal to zero. Applying a gate voltage the Fermi level is shifting near Dirac point to reach electrons or holes. Therefore, any graphene device is ambipolar. Thus, the charge density in graphene is related to the applied gate voltage V_g through by the simple relation:

$$n = \pm \varepsilon_0 \varepsilon_d V_g / te = \pm \alpha V_g \tag{3}$$

where e is the electron charge, and ε_0 and ε_d are the dielectric permittivity of air and SiO_2, respectively. The fact that the gate voltage dictates the carrier density and its type (electrons or holes) is an example of electrical doping, which is typical to nanostructures, having the same role as the chemical doping that is typical for semiconductor devices. However, in contrast to semiconducting devices, where the chemical doping cannot be changed after the fabrication processes, the *p* or *n* doping in graphene can be electrically tuned by applying negative or positive voltages, respectively.

The graphene, in spite of one atom thickness, is visible with a simple optical microscope with an optical filter. An example is given in Fig. 3, where the photos of a graphene monolayer and bilayer stake are displayed by courtesy of Graphene Industries. More details are found in references [17–19]. More precise methods, such as Raman spectroscopy, are able to identify the type of graphene and its thickness [21]. Graphene is a very robust material, in fact the strongest material, with an elastic stiffness of 340 N/m and a Young modulus of 1.5 TPa [22].

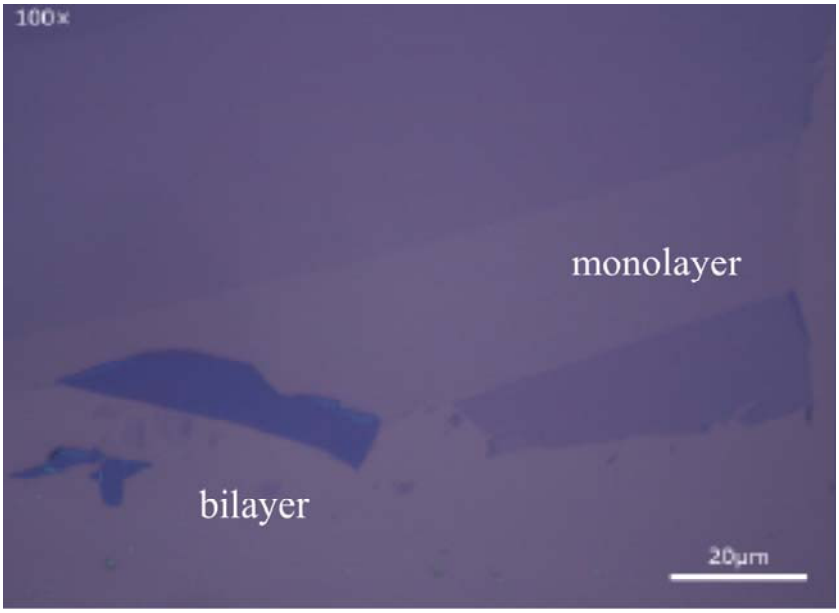

Fig. 3 – Optical picture of graphene bi- and monolayer.

There are many other properties of graphene which make it a unique material, such as very high mobility, unique tunneling behavior (Klein tunnelling) or Hall effect, but they are well described in the review papers mentioned and in particular in [23]. The main properties of graphene are summarized in Table 1.

Table 1

Graphene properties

Parameter	Values	Remarks
Mobility	40 000 $cm^2V^{-1}s^{-1}$	At room temperature (intrinsic mobility 200 000 $cm^2V^{-1}s^{-1}$ in suspended structures)
Mean free path (ballistic transport)	200–300 nm	At room temperature
Fermi velocity	$c/300$=1000000 m/s	At room temperature
Thermal conductivity	5000 W/mK	Better thermal conductivity than in most crystals
Young modulus	1.5 Tpa	Ten times greater than in steel
Mobility	40 000 $cm^2V^{-1}s^{-1}$	At room temperature (intrinsic mobility 200 000 $cm^2V^{-1}s^{-1}$ in suspended structures)

The graphene is now produced at the wafer scale and even larger. Various methods of growth are used to obtained graphene, but the paradox is that still the rough method of exfoliation of graphene from graphite displays best graphene quality. Table 2 summarizes the principal growth techniques and the yield obtained. There are two recent review papers which describes in a very clear manner the graphene growth techniques and the future developments [23, 24]. The most promising method to grow graphene is the CVD, since relatively high mobilities are obtained and the graphene films are fabricated by roll-to-roll techniques up to 30-inch on flexible copper substrates, having applications in flexible electronics, such as touch screens where graphene film is used as a transparent electrode [25]. Noteworthy, graphene is compatible with standard resist processing techniques used frequently for semiconductor devices.

Table 2

Graphene growth methods properties

Material	Method	yield	Graphene surface
Graphite	Repetitive peeling HOPG	low	Small
SiC	Desorption of Si atoms at high temperature	moderate	Moderate (3-4 inches wafers)
GO	GO dispersion into hydrazine	high	Large
CVD	Gas mixture (CH_4 and n H_2)	very high	Very large (30 inches)

The physical of graphene nanoribbons (GNR) and CNTs are not described here, but the Refs. [26, 27, 28] are describing these issues in detail.

3. GRAPHENE DEVICES

Graphene is a hot topic in nanoelectronics, in the area of transistors [29], spin valve devices [30], photodetectors [31], single-electron transistors [32], and solar cells [33]. The main reason is that nowadays the microwave devices and circuits are fabricated up to 100 GHz using GaAs, SiGe, InP, SiGe or high-resistivity Si, which are mature technologies implemented in semiconductor fabrication plants and the search for new materials which could improve the already impressive performances of microwave and millimeterwave devices is not a first priority.

Nananomaterials such as nanoparticles, nanowires, carbon nanotubes or graphene, which now are a hot topics of entire domains such as nanoelectronics, nanomedicine or biology, are not widespread in RF domain despite the fact that important researches regarding CNT microwave devices were recently reported [34], and a revolutionary type of radio termed nanoradio was recently demonstrated [35], and the graphene devices for RF are increasing every year.

A strong reason for the scarce utilization of nanomaterials, in particular CNTs, in microwaves and millimeterwaves is the very large impedance (typically greater than 10 kΩ) displayed by the devices and circuits based on them. So, they are extremely difficult to match with the standard 50 Ω impedance of microwave circuits or equipments. In the case of CNT devices, various methods are used to arrange in parallel thousands of nanotubes [36]. Using this concept, arrangements of thousands of CNT parallel transistors with cutoff frequency of 80 GHz were demonstrated using extremely dense networks of high-purity semiconducting SWCNT [37].

On the other hand, graphene is a planar nanomaterial, and it is another way to replace the SWCNT thin film to reach the desired 50 Ω impedance. We have recently fabricated a coplanar line (CPW) deposited on graphene, we have measured its properties up to 65 GHz, and finally we have determined the equivalent circuit of the CPW [38], which has a resistive part of the impedance of nearly 50 Ω. Our work was used further to measure the quantum oscillations in graphene within the microwave range [39], demonstrating the validity of our concept. The CPW graphene device is displayed in Fig. 4, where the relevant dimensions are marketed on the SEM photo.

Graphene monolayer was fabricated by Graphene Industries and positioned over a 300 nm SiO_2 layer grown on a heavily doped Si substrate. The graphene has rather small dimensions in comparison with the CPW due to the necessity to connect the CPW to the vector network analyzer (VNA) and the typical dimensions of the probe tips, which in our case has a pitch of 150 mm. In Fig. 4, the patterned

three electrodes of CPW are covering entirely the graphene region. Beyond the graphene region we have enlarged the electrodes on the SiO_2 substrate to match the probe tips dimensions, the entire CPW length being 80 μm. The CPW was metalized using the standard lift-off process based on PMMA coating. The spatial coordinates of the graphene were mapped before the utilization of the SEM since the graphene is not visible when coated with PMMA. The PMMA bi-layer was spin coated on the sample and baked in oven at 150ºC. A JEOL 7000F SEM equipped with a RAITH Elphy quantum attachment was subsequently used to pattern the PMMA layer directly with an electron beam. Further, the PMMA layer was developed in MIBK:IPA 1:3 and was subsequently introduced in a Temescal e-gun evaporation chamber where the gold were deposited with the thickness of 300 nm. The lift-off process was completed using acetone to remove the PMMA.

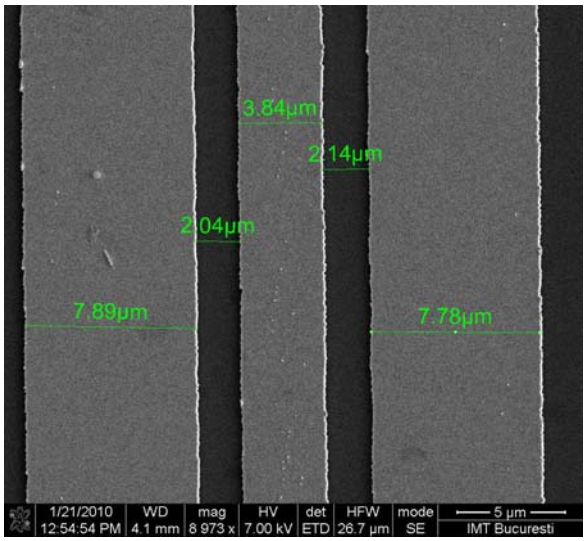

Fig. 4 – The coplanar line on graphene. (Figure reproduced from [38]).

The measurements were done in two situations. We have measured two CPW lines deposited on the same wafer with the same dimensions under the same conditions on a VNA biasing the CPW at various dc voltages. One of these CPW was without graphene while the other is that displayed in Fig. 4, containing graphene under the metallic electrodes as described above. The measurement of the S parameters of both CPW structures has displayed different results. In the case of the CPW deposited on graphene we have seen that the S parameters are shifted as a function of the DC voltage applied on the CPW between the central electrode and its ground electrodes, while in the case of the CPW without graphene this effect was not visible. The S_{21} parameter is displayed in Fig. 5 for the frequency range 5–60 GHz while the bias was varied in the range 0–6 V.

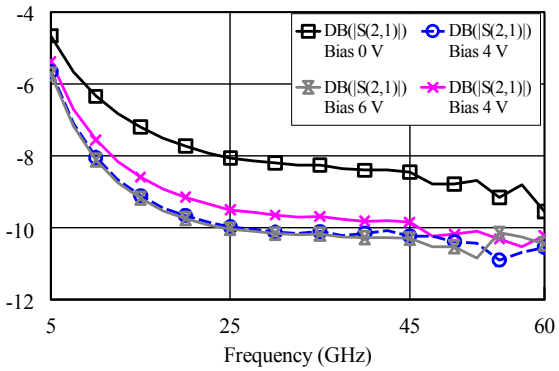

Fig. 5 – The S_{21} parameter of the graphene CPW (figure reproduced from [38]).

We have further extracted an equivalent circuit of graphene CPW using intensive modelling based on MoM (IE3D version) Zeeland Software. A good agreement between the simulated and experimental results were found for the Si permittivity of $\varepsilon_r = 11.9$, a conductivity of 0.05 S/m and a loss tangent of 0.05. The simulations have shown that graphene can be modelled as a parallel lumped circuit connected as an internal port with the CPW electromagnetic model. We have further extracted an equivalent circuit of graphene CPW using intensive modelling based on MoM (IE3D version) Zeeland Software. A good agreement between the simulated and experimental results were found for the Si permittivity of $\varepsilon_r = 11.9$, a conductivity of 0.05 S/m and a loss tangent of 0.05. The simulations have shown that graphene can be modeled as a parallel lumped circuit connected as an internal port with the CPW electromagnetic model. The resistance varied in the range 25–42 Ω for biases between –6 V and 6 V, while the capacitance remains almost constant, around 60 fF as shown in Fig. 6. The almost 50 Ω impedance of graphene is a result of its physical properties. Graphene has a finite conductivity at zero bias, and the conductivity is strongly dependent on the applied voltage. Therefore, in this case it is possible to reach the desired 50 Ω [38, 40].

Graphene microwave and millimeterwave field-effect transistors (FETs) are the most studied graphene devices. The first graphene transistor had a top gate configuration with SiO_2 as dielectric [41]. In the next years, the cut-off of graphene FETs has increased from a few GHz to 100 GHz [42] due to better fabrication technologies, allowing a decrease in the gate length and the use of dielectrics which, when deposited on graphene, do not damage dramatically the graphene. Other early important results regarding FET graphene transistors for microwaves are retrieved in [43–45]. The reference [29] is the most extended review about graphene transistors up to now. Recently, graphene transistors having a nanowire (CO_2Si-Al_2O_3 core-shell nanowire) as a gate and having a cut-off frequency

exceeding 300 GHz were reported [45]. Recently, we have also designed and fabricated an RF graphene transistor [46], having a double-gate electrode configuration which is positioned over graphene, playing the role of a channel, ended with two electrodes: source (S) and drain (D). The gate electrodes are separated from graphene by a thin PMMA layer which does not destroy the graphene lattice. The graphene FET transistor is displayed in Fig. 7. The fabrication of this transistor consists of several steps. A high-quality flake of graphene monolayer was deposited over a 300 nm SiO_2 grown on high-resistivity Si by Graphene Industries obtained by exfoliation from graphite.

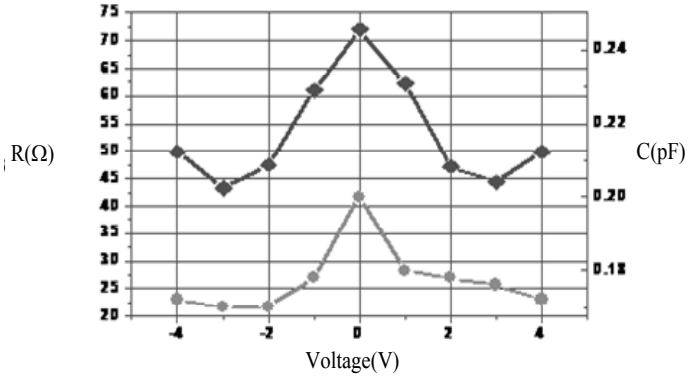

Fig. 6 – The equivalent circuit of CPW graphene up to 60 GHz.

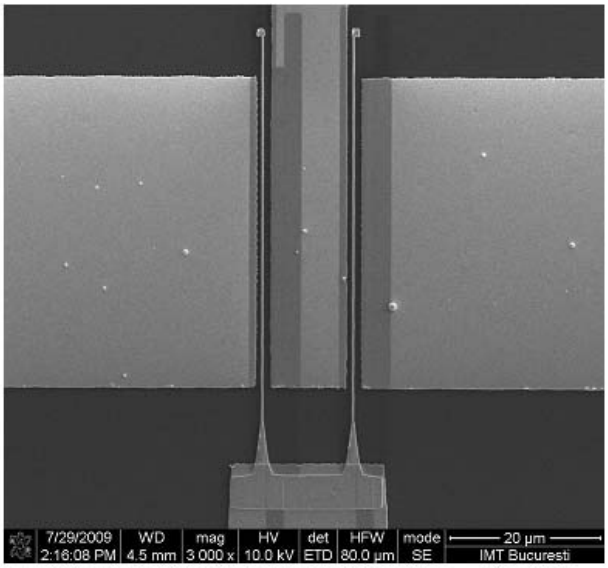

Fig. 7 – Graphene FET with two gates. (Figure reproduced from [46]).

The detailed steps for fabrication of the graphene FET displayed in Fig. 7 are described in detail in [46]. In principle, the fabrication process combines various deposition techniques using electron beam lithography. The gate dielectric is an organic dielectric, a PMMA layer, having a thickness of 200 nm. The dimensions of graphene FET are: gate length L_g = 200 nm, source-drain distance L = 2 μm and source/drain width W = 40 μm. We have measured a maximum stable gain greater than 1 up to 5 GHz, while the cutoff frequency is around 80 GHz. The mobility was determined from the drain current *versus* gate voltage characteristic and was found to be 8 000 cm^2/Vs at room temperature and far from the Dirac point. This value is eight times greater than in silicon. Other characteristics of our FET graphene are found in. It is noteworthy that far from the Dirac point the graphene FET transistor behaves as an active device, *i.e.* amplifies the microwave signals, while at the Dirac point the transistor becomes a passive device, its amplification being suppressed due to carrier recombination. New microwave applications of graphene are multipliers based on the graphene top-gate FET. They were first time reported in [44] but worked at very low frequencies (tens of kHz). Recently, we have shown that the CPW graphene (Fig. 4) is acting as a millimeter frequency multiplier up to 40 GHz [47] due to the strongly nonlinear electromagnetic response of Dirac fermions at relatively low values of electric fields. The experimental set-up is based on a generator in the 1–65 GHz range with controlled output power, delivered directly by the VNA 37397D-Anritsu, and a spectrum analyzer up to 40 GHz. The generator is located at the CPW port, while the spectrum analyzer is located at the other port. The CPW graphene was contacted with RF probe tips. These probe tips were located over the CPW at its input and output, and were further connected by semi-rigid cables to the VNA, acting as generator, and to the spectrum analyzer. Furthermore, in order to control the electromagnetic field propagation, the graphene CPW was biased using the bias tee integrated in the VNA. The output multiplier power P dependence at 5 different frequencies is displayed in Fig. 8. We have to note that the efficiency of the multiplication in our device is low, and this is due to the impedance mismatches at the input and output. This efficiency can be increased up to a typical value of 10 % encountered in Schottky multipliers or even higher, by adding matching circuits at the desired frequencies at the input and output of the device. Our target was to see how many frequencies could be generated rather than to multiply a certain input frequency with a given multiplication factor n, and this first result is very promising since only a single sheet of atoms patterned with metallic electrodes is able to multiply frequencies up to millimeterwave.

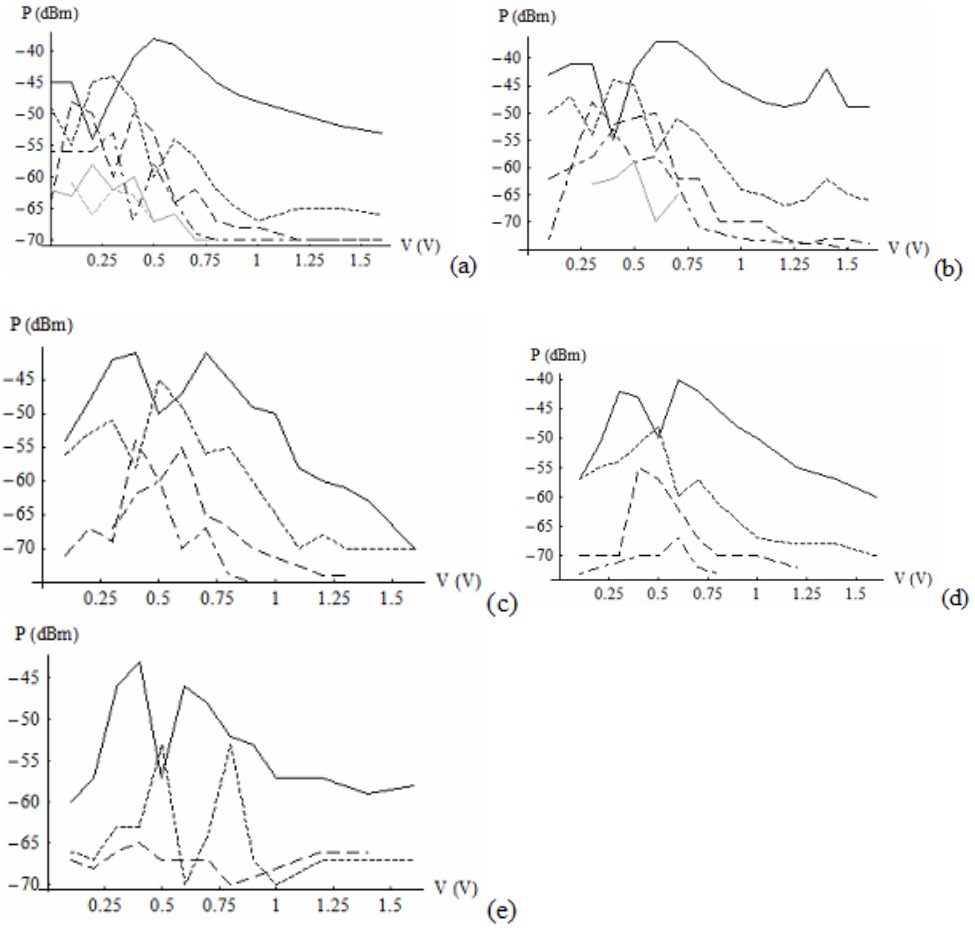

Fig. 8 – Power dependence on dc bias for the second-order (solid line) third-order (dotted line), fourth-order (dashed line), fifth-order (dashed-dotted line), sixth-order (solid gray line), and seventh-order (dotted gray line) harmonics of an excitation frequency of: a) 1 GHz; b) 2 GHz; c) 3 GHz; d) 5 GHz; e) 10 GHz (figure reproduced from [47]).

5. CONCLUSIONS

The high frequency applications of carbon-based materials are of paramount importance in the development of microwaves, photonics, THz electronics, and other related areas. Although the growth of graphene and CNTs, as well as their manipulation, are at the beginning, performances achieved in this area are progressing with an astonishing pace. These conclusions are sustained by the the very recent special issue of Proceedings of IEEE 101 (2013) issue 7 and termed "*Emerging graphene based electronic and photonic devices*".

Acknowledgements. I would like to thank to many scientists which helped me in the quest in the area of carbon nanoelectronics, most of them being co-authors of many papers published in the last period of time. My wife Daniela has helped me with her deep knowledge in the area of quantum mechanics, solid state physics and graphene physics. My colleagues from IMT Bucharest (Alex Muller, Dan Neculoiu, Adrian Dinescu, Alina Cismaru, Antonio Radoi), dr. George Konstantinidis from FORTH Heraklion, dr. George Deligeorgis from LAAS Toulouse were behind almost any device reported in this talk especially due to their invaluable knowledge in the area of semiconductor technology. I am grateful Prof. Hans Hartnagel who during many years has helped and guided me in the area of microwaves and nanoelectronics.

Part of this work was supported by a grant of Romanian National Authority for Scientific Research, CNCS-UEFISCDI, project number PN-II-ID-PCE-2011-3-0071, and the European Commission for the financial support via the FP 7 NANO RF (Grant agreement 318352).

REFERENCES

1. S. E. Thompson and S. Parthasarathy, Elsevier Materials Today, **9**, 20 (2006).
2. S. Iijima, Nature, **354**, 56 (1991)
3. A. K. Geim, *Graphene: Status and Prospects*, Science, **324**, 1530 (2010).
4. A. H. Neto, F. Guinea, N.M.R. Peres, K.S. Novoselov, and A.K. Geim, Rev. Mod. Phys., **81**,109 (2009).
5. T. Palacios, A. Hsu, and H. Wang, IEEE Communications Magazine, **5**, 122 (2010).
6. J. Moon, D. Curtis, M. Hu, D. Wong, C. McGuire, P. Campbell, G. Jernigan, J. Tedesco, B. VanMil, R. Myers-Ward, C. Eddy, and D. Gaskill, IEEE Electron Devices Lett., **30**, 650 (2009).
7. X. Li, W. Cai, J. An, S. Kim, J. Nah, D. Yang, R. Piner, A.Velamakanni, I. Jung, E. Tutuc et al., *Large-area synthesis of high quality and uniform graphene films on copper foils*, Science, **324**,1312 (2009).
8. G. W. Hanson, J. Appl. Phys., **104**, 084 314 (2008).
9. D. Mencarelli, T. Rozzi, and L. Pierantoni, Nanotechnology, **21**,155701–155710 (2010).
10. V. Gouttenoire, T. Barois, S. Perisanu, J.-L. Leclercq, S. T. Purcell, P. Vincent, and A. Ayari, Small, **6**, 1060 (2010).
11. A.K. Naik, M.S. Hanay, W.K. Hiebert, X.L. Feng, and M.L. Roukes, Nature Nanotechnology, **4**, 445 (2009).
12. A.K. Geim, K.S. Novoselov, Nature Materials, **6**, 183 (2007).
13. K.S. Novoselov, A.K. Geim, S.V. Morozov, D. Jiang, Y. Zhang, S.V. Dubonos, I.V. Grigorieva, A.A. Firsov, Science, **306**, 666 (2004).
14. W. Bao, F. Miao, Z. Chen, H. Zhang, W. Jang, C. Dames and C.N. Lau, Nature Nanotechnology, **4**, 562 (2009).
15. M. Dragoman, D. Dragoman, *Nanoelectronics. Principles and Devices*, Artech House, 2009.
16. A.H. Castro Neto, F. Guinea, N.M.R. Peres, K.S. Novoselov and A.K. Geim, Rev. Mod. Phys., **81**, 109, 2009.
17. P. Blake, E.W. Hill, A.H. Castro Neto, K.S. Novoselov, D. Jiang, R. Yang, T.J. Booth, A.K. Geim, Appl. Phys. Lett., **91**, 063124 (2007).
18. D.S. Abergel, A. Russel, and V.I. Falko, Appl. Phys. Lett., **91**, 063125 (2007).
19. J. Kim, F. Kim, and J. Huang, Materials Today, **13**, (2010).
20. A.C. Ferrari, J.C. Meyer, V. Scardaci, C. Casiraghi, M. Lazzeri, F. Mauri, S. Piscanec, D. Jiang, K.S. Novoselov, S. Roth and A. Geim, Phys. Rev. Lett., **18**, 187401 (2006).
21. Z.H. Ni, H.M. Wang, J. Kasim, H.M. Fan, T. Yu, Y.H. Wu, Y.P. Feng, and Z.X. Shen, Nano Letters, **7**, (2007).
22. C. Lee, X. Wei, J.W. Kysar, J. Hone, Science, **321**, 385 (2008).
23. C. Soladano, A. Mahmood, and E. Dujardin, Carbon, **48**, 2127 (2010).

24. Y.T. Wu, T. Yu, and Z.X. She, J. Appl. Phys., **108**, 071301 (2010).
25. J.H. Ahn, B.H. Hong, S. Bae, H. Kim, Y. Lee, X. Xu, J.-S. Park, Y. Zheng, J. Balakrishnan, T. Lei, H.R. Kim, Y II Song, Y.-J. Kim, K.S. Kim, B. Ozyilmaz, S. Iijima, Nature Nanotechnology, **5**, *6*, 574 (2010).
26. M. Y. Han, B. Ozyilmaz, Y. Zhang, and P. Kim, Phys. Rev. Lett., **98**, 206 (2007).
27. F. Leonard, *The physics of carbon nanotubes*, William Andrew, Nordwich, 2009.
28. E. Joselevich, H. Dai, J. Liu, K. Hata, A.H. Windle, *Carbon synthesis and organization*, in *Carbon Nonotubes. Advanced Topics in Synthesis, Structure, Properties and Applications,* A. Jorio, G. Dresselhaus, M.S. Dresselhaus (Eds.), Springer; Topics in Applied Physics, **111**, 101–164, 2008.
29. F. Schwierz, Nanotechnology, **5**, 487(2010).
30. E.W. Hill, A.K. Geim, K. Novoselov, F. Schedin, P. Blake, IEEE Trans. On Magnetics, **42**, 2644 (2006).
31. T. Mueller, F. Xia, and P. Avouris, Nature Photonics, **4**, 297 (2010).
32. T. Ihn, J. Günttinger, F. Molitor, E. Schurtenberg, A. Jacobson, A. Hellmüller, T. Frey, S. Dröscher, C. Stampfer, E. Ensslin, Materials Today, **13**, 44 (2010).
33. J. Wu, H. A. Becerril, Z. Bao, Z. Liu, Y. Chen, and P. Peumans, Appl. Phys. Lett., **92**, 263302 (2008).
34. C. Rutherglen, D. Jain and P. Burke, Nature Nanotechnology, **4**, 811(2009).
35. K. Jensen, J. Weldon, H. Garcia, and A. Zettl, Nano Letters, **7**, 3508 (2007).
36. C. Rutherglen, D. Jain, and P. Burke, Appl. Phys. Lett., **93**, 083119(2008).
37. L. Nougaret, H. Happy, G. Dambrine, V. Derycke, J. -P. Bourgoin, A.A. Green, M.C. Hersam, Appl. Phys. Lett., **94**, 243505/1-3 (2009).
38. G. Deligeorgis, M. Dragoman, D. Neculoiu, D. Dragoman, G. Konstantinidis, A. Cismaru, and R.Plana, Appl. Physics Letters, 073107 (2009).
39. P. Jiang, A.F. Young, W. Chang, P. Kim, L.W. Engel, and T.C. Tsui, Appl. Phys. Lett., **97**, 062113 (2010).
40. D. Neculoiu, G. Deligeorgis, M. Dragoman, D. Dragoman, G. Konstantinidis, A. Cismaru, and R. Plana, *Electromagnetic propagation of graphene in the mm-wave frequency rang*e, European Microwave conference, Sept. 2010, Paris, France.
41. M.C. Lemme, T. Echtermayer, M. Baus, H. Kurz, IEEE Electron Device Letters, **282** (2007).
42. W. Lin, C. Dimitrakopoulos, K.A. Jenkins, D.-B. Farmer, H.Y.-Chiu, A. Grill, and P. Avouris, Science, **327**, 662 (2010)
43. I. Meric, M.Y. Han, A.F. Young, B. Ozyilmaz, P. Kim and K.L. Shepard, Nature Nanotechnology, **3**, 654 (2008).
44. H. Wang, D. Nezich, J. Kong, and T. Palacios, IEEE Electron Dev. Lett., **30**, 547 (2009).
45. L. Liao, Y.-C. Lin, M. Bao, R. Cheng, J. Bai, Y. Liu, Y. Qu, K.L. Wang, Y. Huang, X. Duan, Nature, **467**, 305 (2010).
46. G. Deligeorgis, M. Dragoman, D. Neculoiu, D. Dragoman, G. Konstantinidis, A. Cismaru, and R. Plana, Appl. Phys. Lett., **96**, 103105 (2010).
47. M. Dragoman, D. Neculoiu, G. Deligeorgis , G. Konstantinidis, D. Dragoman, A. Cismaru, A.A. Muller, R. Plana, Appl. Phys. Lett. Appl. Phys. Lett., **97**, 09310 (2010).